Nanoscale

COMMUNICATION

View Article Online
View Journal | View Issue

Cite this: *Nanoscale*, 2016, **8**, 12520

Received 10th December 2015,
Accepted 7th January 2016

DOI: 10.1039/c5nr08782a

www.rsc.org/nanoscale

A highly fluorescent AIE-active theranostic agent with anti-tumor activity to specific cancer cells†

Yueyue Zhao,‡[a,b] Ryan T. K. Kwok,‡[a,b] Jacky W. Y. Lam[a,b] and Ben Zhong Tang*[a,b,c]

A tetraphenylethene derivative with a structure resembling Tamoxifen is designed and synthesized as a theranostic agent for cell imaging and anti-breast cancer therapy. Its high brightness, excellent photostability and long-term cell tracing properties enable elucidation of its working mechanism and hence provide new insights into drug development.

Among various diseases, cancer is the most difficult one to cure and a leading cause for morbidity and mortality.[1] Every year, approximately 14 million new cases worldwide have been emerging. Thus, gaining more knowledge on such disease will aid in discovering and developing new, safe and effective cancer drugs.[2,3] Unfortunately, the development of drugs especially those for cancer is a lengthy, high-risk and costly process as it involves many stages of drug screening and clinical trials. A slight difference in the molecular structures of drugs may bring a great impact on their curing effects. For instance, small molecular drugs usually exert their effects by binding to one or a few protein targets. Such critical interactions, however, are hard to follow and study in live cells or entire organisms due to the lack of indication from the drug-target conjugates. In this regard, the development of theranostic drugs, which combines both therapeutic and diagnostic capabilities, is one of the most popular research studies in clinical fields. The integration of diagnostic imaging capability with therapeutic intervention allows the drug to be targeted and monitored together, enabling the assessment of drug distribution and release, and the evaluation of the drug response and efficacy all in a non-invasive and real-time fashion.[4–6]

Tamoxifen (TMX; Scheme 1) is pharmacologically classified as a selective modulator of estrogen receptor (ER) for treating breast cancer. It is commonly used as chemotherapeutic agent for curing ~70% patients with ER+ breast cancer. Yet, only a few studies have been carried out to investigate how TMX distributes and functions at the cellular level. It is postulated that TMX acts as an estrogen competitor, which binds to the ER on tumors. This forms a drug-acceptor complex, whose entrance to the nuclear complex prevents the gene expression and leads to the inhibition of the estrogenic effects.[7–9] However, TMX itself shows weak emission, and thus it is difficult to study the exact working principle visually. Recently, TMX has been reported to induce autophagy in breast cancer cells.[10,11] However, the use of such a process in cancer treatment still remains unclear. Thus, the development of anti-breast tumor agents that can follow and monitor their response will play an essential role to formulate effective treatment course and elucidate their working mechanisms.

The challenges of meeting the expectations in some desired target products complicate the drug discovery process. On careful examination of the chemical structure of TMX, we found that it is a structural analogue of tetraphenylethene (TPE), an iconic fluorogen exhibiting aggregation-induced emission (AIE) features. TPE exhibits no emission in solution

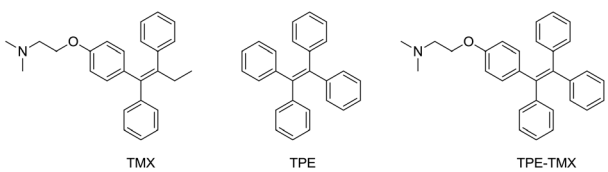

Scheme 1 Molecular structures of Tamoxifen (TMX), tetraphenylethene (TPE) and TPE–TMX.

[a]*HKUST Shenzhen Research Institute, No. 9 Yuexing 1st Road, South Area, Hi-tech Park, Nanshan, Shenzhen 518057, China. E-mail: tangbenz@ust.hk*
[b]*Department of Chemistry, Hong Kong Branch of Chinese National Engineering Research Center for Tissue Restoration and Reconstruction, Institute for Advanced Study, Division of Biomedical Engineering, Division of Life Science, State Key Laboratory of Molecular Neuroscience, Institute of Molecular Functional Materials, The Hong Kong University of Science and Technology, Clear Water Bay, Kowloon, Hong Kong, China*
[c]*Guangdong Innovative Research Team, SCUT-HKUST Joint Research Laboratory, State Key Laboratory of Luminescent Materials and Devices, South China University of Technology, Guangzhou 510640, China*
†Electronic supplementary information (ESI) available: Detailed synthesis and characterization of TPE–OH and TPE–TMX; PL spectra of TPE–TMX; fluorescent photographs of TPE–TMX taken under UV irradiation; various concentrations of TPE–TMX with different incubation times. See DOI: 10.1039/c5nr08782a
‡These authors contributed equally to this work.

due to the active intramolecular rotation and vibration, which serves as a relaxation channel for the excited states to deactivate nonradiatively. In the aggregated state, such motions are restricted due to the steric hindrance between the molecules. This blocks the nonradiative pathway but opens the radiative decay channel, thus enabling the fluorogen to show strong fluorescence upon photoexcitation.[12,13] By taking such a unique AIE feature, a variety of TPE derivatives have been developed and various biological applications such as cell imaging and turn-on detection of biomacromolecules have been found.[14–17]

Inspired by the similarity in structure between TMX and TPE, in this work, we attempted to modify TMX by replacing its ethyl group with a phenyl group. We explored the capability of the resulting fluorogen (TPE–TMX; Scheme 1) as a theranostic agent for imaging and treatment of breast cancer. Herein, we demonstrate that TPE–TMX could image and show a therapeutic response to ER+ breast cancer cells with high specificity, suggesting its potential usage as theranostic drugs for breast cancer therapy. Its high brightness and excellent photostability properties endow it with long-term cell tracing ability, which enables us to understand the drug action and provides new insights into drug development.

TPE–TMX was prepared and synthesized by the synthetic route as depicted in Scheme S1 in the ESI.† The intermediate (TPE–OH) was prepared by McMurry coupling of benzophenone and 4-hydroxylbenzophenone catalyzed by zinc and $TiCl_4$. Further treatment of TPE–OH with 2-bromo-*N*,*N*-dimethylethanamine under basic conditions furnished the desirable product TPE–TMX. Its molecular structure was characterized by ^{1}H NMR, ^{13}C NMR and mass spectroscopy with satisfactory results (Fig. S1–S3†). Like other TPE derivatives, TPE–TMX exhibits AIE characteristics. It shows almost no emission in pure THF solution. Addition of water, a poor solvent for the fluorogen, into its THF solution induces the emergence of an emission peak at 380 nm, whose intensity becomes higher progressively with increasing the water content. At a high water content, an additional signal at 480 nm corresponding to TPE aggregates is also detected. The emission at a 95% water fraction is so strong that its intensity is about 125-fold higher than that in the pure THF solution (Fig. S4†).

To explore the capability of TPE–TMX as a theranostic agent for imaging and treatment of breast cancer, we first compared the behavior of TPE–TMX with TMX in breast cancer cells. In this study, the human mammalian cancer cell line (MCF-7) is employed, which is known to grow estrogen dependently and is widely used to study the anti-estrogen effect. MCF-7 cells are incubated in Dulbecco's Modified Eagle's Medium (DMEM) with TPE–TMX (2 μM) and TMX (2 μM) for 24 h, respectively. The cells are washed with phosphate-buffered saline (PBS) and then observed under a fluorescence microscope without fixation. Careful observation of the bright-field images in Fig. 1C and G show that many small black dots appear near the nuclei of the MCF-7 cells treated with TMX or TPE–TMX. A few dots, however, are only observed in the untreated MCF-7 cells (Fig. 1A). This result suggests that the

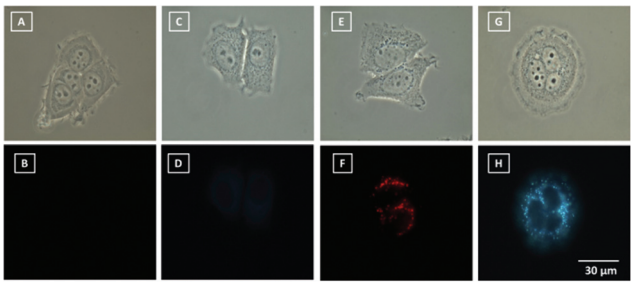

Fig. 1 (A, C, E and G) Bright-field and (B, D, F and H) fluorescent images of MCF-7 breast cancer cells treated with (A and B) buffer solution, (C and D) TMX, (E and F) a mixture of TMX and LysoTracker Red DND-99 (LTR), and (G and H) TPE–TMX. Concentration: TMX (2 μM), LTR (50 nM) and TPE–TMX (2 μM); excitation wavelength: 330–385 nm. All images share the same scale bar: 30 μm.

black dots may originate from the dye molecules or autolysosomes formed due to the presence of dye molecules. The exact intracellular location of TMX, however, cannot be visualized by fluorescence microscopy because it is a weakly emissive emitter (Fig. 1D and S5†). As a result, we used LysoTracker Red DND-99 (LTR), a commercial lysosome specific dye, to co-stain the MCF-7 cells with TMX. Results show that the red fluorescence of LTR is detected in areas correlated well with the location of the black dots (Fig. 1E and F), suggesting that TMX is a lysosome targeting drug. On the other hand, due to the AIE nature of TPE–TMX, its aggregates alone can endow the MCF-7 cells with intense blue emission (Fig. 1H). To verify the subcellular distribution of TPE–TMX, LTR is applied after the MCF-7 cells are stained with TPE–TMX. By varying the excitation wavelength, we found that the dots stained with TPE–TMX also showed red fluorescence of LTR (Fig. 2B and C). The overlay fluorescent image demonstrates excellent co-localization between the fluorescence of LTR and TPE–TMX with a Pearson correlation coefficient of 0.96 (Fig. 2D), indicating that TPE–TMX can selectively stain the autolysosomes in live MCF-7 cells.

Now, it now becomes clear that TPE–TMX, similar to TMX, can target the autolysosomes with high specificity. The next question is: does it possess the same therapeutic ability as that of TMX? To answer this question, we investigated the cytotoxicity of TPE–TMX to different cell lines by the 3-(4,5-dimethyl-

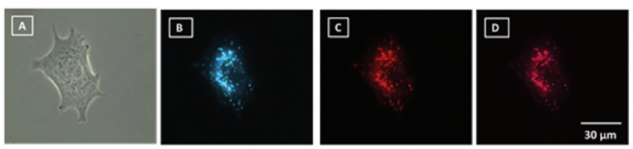

Fig. 2 (A) Bright-field and (B and C) fluorescent images of MCF-7 breast cancer cells stained with LTR (50 nM) for 15 min after being treated with TPE–TMX (2 μM). (D) The merged image of (B) and (C). Excitation wavelength (nm): (B) 330–385 and (C) 520–560. All images share the same scale bar: 30 μm.

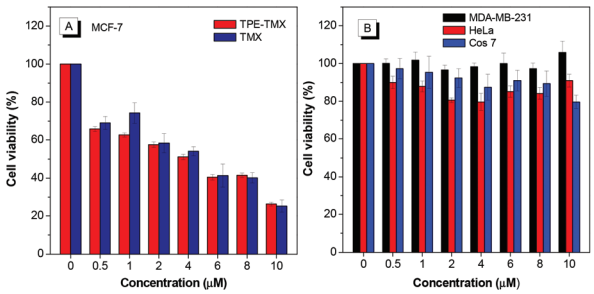

Fig. 3 (A) Cell viability of MCF-7 cells incubated with different concentrations of TPE–TMX and TMX. (B) Cell viability of different cells in the presence of TPE–TMX with different concentrations.

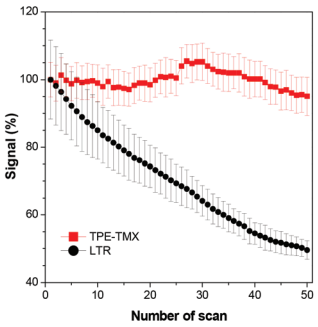

Fig. 4 Loss in fluorescence of MCF-7 cells stained with TPE–TMX and LTR with the number of scan. Excitation wavelength (nm): 405 (TPE–TMX) and 561 (LTR); emission filter (nm): 450–750 (TPE–TMX) and 580–750 (LTR). Irradiation time: 3.58 s per scan. Laser power: 0.1 mW.

thiazol-2-yl)-2,5-diphenyltetrazolium bromide (MTT) assay. As depicted in Fig. 3, TPE–TMX shows only a therapeutic response in the presence of ER+ MCF-7 breast cancer cells. The higher the dose of TPE–TMX used, the lesser the amount of cancer cells survived. Such a response was similar to TMX (Fig. 3A). The cell viability of other cell lines, including MDA-MB-231, an ER– breast cancer cell, changes little even at a high TPE–TMX concentration of 10 μM (Fig. 3B). Such a high specificity may be due to the existence of ERs on MCF-7 cells and such complexation may lead to cell death. To examine whether this hypothesis is true, the fluorescent images of different cells after being treated with 2 μM TPE–TMX for 24 h were taken and examined. The lysosomes in all the tested cells are visualized by the blue fluorescence of TPE–TMX, with those in the MCF-7 cells showing a much stronger fluorescence intensity (Fig. S6†). More interestingly, vacuole formation, swelling of lysosomes and population loss are observed in the image of MCF-7 cells, whereas no obvious morphological change is found in other cell lines. These results demonstrate that TPE–TMX is a promising theranostic agent for ER+ breast cancer cells.

Fluorescent agents with good photostability and long-term tracking ability are highly pursued to elucidate the working mechanisms of cancer drugs. To quantitatively investigate the photo-bleaching resistance of TPE–TMX and LTR, continuous scanning of their stained MCF-7 cells by lasers was carried out and their fluorescence intensity at each scan was recorded. Two sets of MCF-7 cells were first incubated in DMEM for 24 h and then stained with TPE–TMX (2 μM) and LTR (2 μM) for 30 min, respectively. The excitation power from 405 nm and 561 nm channels of the microscope was unified as 0.1 mW. The initial fluorescence intensity of the stained cells was normalized and the percentage of fluorescence intensity loss was calculated. As shown in Fig. 4, no significant signal loss is observed in the TPE–TMX stained cells after 50 scans in a total irradiation time of 3 min. In contrast, more than half of its fluorescence is lost for LTR, indicating that TPE–TMX shows a much higher photobleaching resistance than LTR.

Fluorescent dyes that can retain in viable cells for a long period of time can provide more insights into the functioning of cancer drugs. However, only a few conventional dyes can retain in living cells after several passages. For example, the red fluorescence of cells stained with LTR is dramatically weakened with time and almost no emission is recorded after 72 h (Fig. S7†). In sharp contrast, TPE–TMX behaves differently. Rather than weakening, the fluorescence of TPE–TMX stained cells is strengthened with increasing the number of passages. This may be due to the formation and accumulation of autolysosomes in response to the therapeutic effect of TPE–TMX. Similar to Fig. S6A and S6B,† swelling of lysosomes and population loss are observed in cells as time elapsed after the staining process (Fig. 5A–F; for a more complete set of photos, see Fig. S8†). Except the nuclei, almost the whole MCF-7 cells were emissive after 192 h. Such observation contradicts the commonly accepted working mechanism of TMX, in which the formation of the TMX–receptor complex and its entry to the cell nucleus cause the therapeutic effect. Instead, we propose that TPE–TMX, with the therapeutic effect similar to TMX, can act as an estrogen competitor that binds to ER to form a drug–ER complex. Therefore, less estrogen is able to bind ER. With the shortage of the estrogen–ER complex, the cells become unhealthy. This may activate the process of cell death, leading to an increased number of autolysosomes and hence autophagy and cell ablation.[18–21] On the other hand, the amino group of TPE–TMX allows it to target the lysosome selectively.

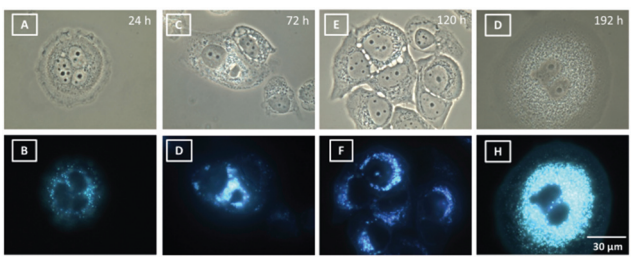

Fig. 5 (A–D) Bright-field and (E–H) fluorescent images of MCF-7 cells taken at different times after being treated with TPE–TMX (2 μM). Excitation wavelength: 330–385 nm. All images have the same scale bar: 30 μm.

Once the molecules accumulate on the surface of lysosomes, their intramolecular motion is restricted, which consequently lights up the lysosomes in cells. This is the first time it is proposed that autophagy can be monitored by fluorescence spectroscopy using a theranostic agent for breast cancer cells.

In summary, a novel theranostic agent for imaging and treatment of ER+ breast cancer cells is developed. Thanks to its easy synthesis, superior photostability and long-term tracing feature, TPE–TMX has been successfully applied for *in situ* and *in vitro* tracking of drug distribution and cancer therapeutic efficacy in living cells. Experimental results show that the induction of autophagy in breast cancer cells by TPE–TMX seems to be the real working principle for its therapeutic effect. Thus, the present work is anticipated to open a new avenue for pharmacokinetics and pharmacodynamics of drug development.

Acknowledgements

This work was partially supported by the National Basic Research Program of China (973 Program, 2013CB834701 and 2013CB834702), the University Grants Committee of Hong Kong (AoE/P-03/08), the Innovation and Technology Commission (ITC-CNERC14SC01) and the Research Grants Council of Hong Kong (16301614, 16301615 and N_HKUST604/14).

Notes and references

1 R. Siegel, J. Ma, Z. Zou and A. Jemal, *CA-Cancer J. Clin.*, 2014, **64**, 9–29.
2 N. H. William, *Nat. Rev. Drug Discovery*, 2010, **9**, 253–254.
3 C. Gorrini, I. S. Harris and T. W. Mak, *Nat. Rev. Drug Discovery*, 2013, **12**, 931–947.
4 M. Hilvo, C. Denkert, L. Lehtinen, B. Muller, S. Brockmoller, T. Seppanen-Laakso, J. Budczies, E. Bucher, L. Yetukurl, S. Castillo, E. Berg, H. Nygren, M. Sysi-Aho, J. Griffin, O. Fiehn, S. Loibl, C. Richter-Ehrenstein, C. Radke, T. Hyotylainen, K. IIjin and M. Oresic, *Cancer Res.*, 2011, **71**, 3236–3245.
5 T. W. B. Liu, J. Chen, L. Burgess, W. Cao, J. Shi, B. Wilson and G. Zheng, *Theranostics*, 2011, **1**, 352–354.
6 K. Yang, L. Feng, X. Shi and Z. Liu, *Chem. Soc. Rev.*, 2013, **42**, 530–547.
7 S. S. Legha, *Ann. Intern. Med.*, 1988, **109**, 219–288.
8 A. Lykkesfeldt, J. Larsen, I. Christensen and P. Briand, *Br. J. Cancer*, 1984, **49**, 717–722.
9 L. Donnelly, D. Evans, J. Wiseman, J. Fox, R. Greenhalgh, J. Affen, I. Juraskova, P. Stavrinos, S. Dawe, J. Cuzick and A. Howell, *Br. J. Cancer*, 2014, **110**, 1681–1687.
10 W. Bursch, A. Ellinger, H. Kienzl, L. Torok, S. Pandey, M. Sikorska, R. Walker and R. S. Hermann, *Carcinogenesis*, 1996, **17**, 1595–1607.
11 A. Bilir, M. A. Altinoz, M. Erkan, V. Ozmen and A. Aydiner, *Pathobiology*, 2001, **69**, 120–126.
12 J. Luo, Z. Xie, J. W. Y. Lam, Y. Dong, S. M. F. Lo, I. D. Williams, D. Zhu and B. Z. Tang, *Chem. Commun.*, 2001, 1740–1741.
13 Y. Hong, J. W. Y. Lam and B. Z. Tang, *Chem. Soc. Rev.*, 2011, **40**, 5361–5388.
14 J. Mei, Y. Hong, J. W. Y. Lam, A. Qin, Y. Tang and B. Z. Tang, *Adv. Mater.*, 2014, **26**, 5429–5479.
15 R. T. K. Kwok, C. W. T. Leung, J. W. Y. Lam and B. Z. Tang, *Chem. Soc. Rev.*, 2015, **44**, 4228–4238.
16 D. Ding, K. Li, B. Liu and B. Z. Tang, *Acc. Chem. Res.*, 2013, **46**, 2441–2453.
17 D. Ding, J. Liu, G. Feng, K. Li, Y. Hu and B. Liu, *Small*, 2013, **9**, 3093–3102.
18 D. Glick, S. Barth and K. F. Macleod, *J. Pathol.*, 2010, **221**, 3–12.
19 S. Suman, T. Das, R. Reddy, A. Nyakeriga, J. Luevano, D. Konwar, P. Pahari and C. Damodaran, *Br. J. Cancer*, 2014, **111**, 309–312.
20 P. Medina, S. Silvente-Poirot and M. Poirot, *Autophagy*, 2009, **5**, 1066–1067.
21 K. Cho, Y. Yoon, J. Choi, S. Lee and J. Koh, *IOVS*, 2012, **53**, 5344–5353.